

# Synthesis, Micellization, and Surface Activity of Novel Linear-Dendritic Carboxylate Surfactants

Yuning Lou<sup>1#</sup> · Yajuan Dong<sup>1#</sup> · Xiaoyong Wang<sup>1</sup>  · Feirong Gong<sup>2</sup> · Min Zhao<sup>1</sup> · Zongming Rong<sup>1</sup>

Received: 18 January 2020 / Revised: 14 June 2020 / Accepted: 17 July 2020  
© 2020 AOCS

**Abstract** Two generations of novel linear-dendritic carboxylate surfactants  $C_{18}\text{-G}_1\text{-(COONa)}_2$  and  $C_{18}\text{-G}_2\text{-(COONa)}_4$  have been synthesized by the divergent method and their structures are characterized by  $^1\text{H}$  Nuclear Magnetic Resonance and Infrared analysis. The electrical conductivity measurement is used to measure the Krafft temperatures of  $C_{18}\text{-G}_1\text{-(COONa)}_2$  and  $C_{18}\text{-G}_2\text{-(COONa)}_4$ , which are much smaller than those of the corresponding conventional surfactant sodium stearate. The markedly enhanced solubility of two linear-dendritic surfactants is ascribed to the high hydrophilicity of surfactant headgroups induced by the carboxylate and ester groups. The critical micelle concentration (CMC) values obtained from both the electrical conductivity and surface tension measurements indicate that the micellizations of linear-dendritic surfactants become favorable with the increase in the number of the surfactant headgroup. However, the surface activity parameters including the surface tension at the CMC, maximum surface excess, and minimum surface area reveal that  $C_{18}\text{-G}_1\text{-(COONa)}_2$  exhibits greater efficiency in

absorbing at the air/water interface compared to  $C_{18}\text{-G}_2\text{-(COONa)}_4$ , owing to their different steric repulsions of the surfactant headgroups. In addition,  $C_{18}\text{-G}_1\text{-(COONa)}_2$  and  $C_{18}\text{-G}_2\text{-(COONa)}_4$  have higher emulsifying ability than the conventional surfactants sodium stearate and sodium octadecyl sulfate.

**Keywords** Linear-dendritic surfactant · Krafft temperature · Micellization · Electrical conductivity · Surface tension

*J Surfact Deterg* (2020).

## Introduction

The possibilities of varying headgroup-tail architecture to design novel types of surfactants have drawn increasing attention both in industrial and academic fields (Asadov et al., 2019a; Mirgorodskaya et al., 2018; Naves et al., 2013). Dendritic surfactants usually have one hydrophobic or hydrophilic chain connecting with the divergent groups like branches, where the number of branched groups arranged in a neat way can increase as the surfactant generation increases (Shavykin et al., 2018). The unique structure causes dendritic surfactants to have special aggregation behaviors in the solution and at the interface, together with varied advantages such as controllable molecular structure, geometric symmetry of molecular configuration, variable types, and number of functional groups (Suek and Lamm, 2008). The surfactants containing the dendritic polymeric structures have been widely investigated in the synthesis, aggregation, and application properties (Gosika et al., 2019; Tian et al., 2019).

✉ Xiaoyong Wang  
xiaoyong@ecust.edu.cn

✉ Feirong Gong  
gongfeirong@ecust.edu.cn

✉ Min Zhao  
zhaomin6502@sina.com

<sup>1</sup> School of Chemistry & Molecular Engineering, East China University of Science and Technology, Shanghai, 200237, China

<sup>2</sup> School of Materials Science & Engineering, East China University of Science and Technology, Shanghai, 200237, China

Present address: Yajuan Dong, Enkun Chemical Co., Ltd. Shanghai, Shanghai 200444, China

<sup>#</sup>These two co-first authors contributed equally to this work.

Compared to dendritic polymeric surfactants with relatively high polydispersity, dendritic surfactants with low molecular weight have the fixed molecular mass, high solubility capacity, and easily controlled aggregation behaviors. Polypeptides can be thought as dendritic molecules, carrying a long carbon chain on which different functional groups are grafted (Jacobs et al., 2014). Actually, some surfactants commonly studied such as sodium bis(2-ethylhexyl) sulfosuccinate and Gemini surfactants have branched structures in their headgroups or hydrophobic tails, which brings about many unique properties superior to those of the surfactants carrying one headgroup and one alkyl chain (Allen et al., 2019; Franke and Rehage, 2019a). The surfactants with multiple headgroups by grafting a dendritic unit of poly(amidoamine) onto an octadecyl chain have been synthesized, which could spontaneously form vesicles in aqueous solutions at  $\text{pH} > 5$  (Wang et al., 2008). The branched and multiheaded surfactants can be considered as the first generation of linear-dendritic surfactants. However, linear-dendritic surfactants with the strict symmetric configuration have not been reported, most probably due to the lack of the controlled synthetic procedures.

Fatty acids and their salts are surface-active materials, which are known as the soap components for over 4000 years (Zaidi et al., 2018). Currently, fatty acid compounds are widely used in daily cosmetics, drug encapsulation, and the construction of high-porosity materials. However, the application of fatty acid compounds are somewhat limited by the low solubility especially for the compounds with the long and saturated alkyl chain (Khuwijitjaru et al., 2002). Sodium stearate, for example, has a high Krafft temperature over  $60^\circ\text{C}$ , and is almost insoluble in water at room temperature. Some approaches such as introducing hydrophilic units such as oxyethylene into the hydrocarbon chain or hydrophilic headgroup provide good water solubility for fatty acid compounds (Liu et al., 2008; Voutsas et al., 2002). Recently, Bhattacharya et al. found that the multiheaded surfactant has the decreased Krafft temperature, owing to the strong interaction between water and the large surfactant hydrophilic part (Bhattacharya and Samanta, 2011).

In order to obtain suitable biodegradable and biocompatible drug carrier, our group previously synthesized a series of linear-dendritic block copolymers consisting of linear poly(ethylene glycol) and comb-like poly(L-lactide) (Gong et al., 2009). Based on the process used for preparing the linear-dendritic block copolymers, the present work gives a convenient synthetic route for two generations of novel linear-dendritic carboxylate surfactants  $\text{C}_{18}\text{-G}_1\text{-(COONa)}_2$  and  $\text{C}_{18}\text{-G}_2\text{-(COONa)}_4$ , holding a hydrophobic linear alkyl chain connected with two and four carboxylate headgroups, respectively. The structures of  $\text{C}_{18}\text{-G}_1\text{-(COONa)}_2$  and

$\text{C}_{18}\text{-G}_2\text{-(COONa)}_4$  have been characterized by  $^1\text{H}$  NMR and IR analysis. The electrical conductivity measurement is used to determine the Krafft temperatures of  $\text{C}_{18}\text{-G}_1\text{-(COONa)}_2$  and  $\text{C}_{18}\text{-G}_2\text{-(COONa)}_4$ , together with sodium stearate for comparison. From the critical micelle concentrations (CMC) determined conductometrically at various temperatures, the relative changes in Gibbs energy of surfactant micellization are evaluated. The surface tension measurement is further employed to study the surface properties of  $\text{C}_{18}\text{-G}_1\text{-(COONa)}_2$  and  $\text{C}_{18}\text{-G}_2\text{-(COONa)}_4$ . Finally, the emulsifying ability of  $\text{C}_{18}\text{-G}_1\text{-(COONa)}_2$  and  $\text{C}_{18}\text{-G}_2\text{-(COONa)}_4$  is measured in comparison with the conventional surfactants sodium stearate and sodium octadecyl sulfate. These studies are intended to deeply understand how the dendritic headgroup influences the solubility, micellization, and surface activity of novel linear-dendritic surfactants.

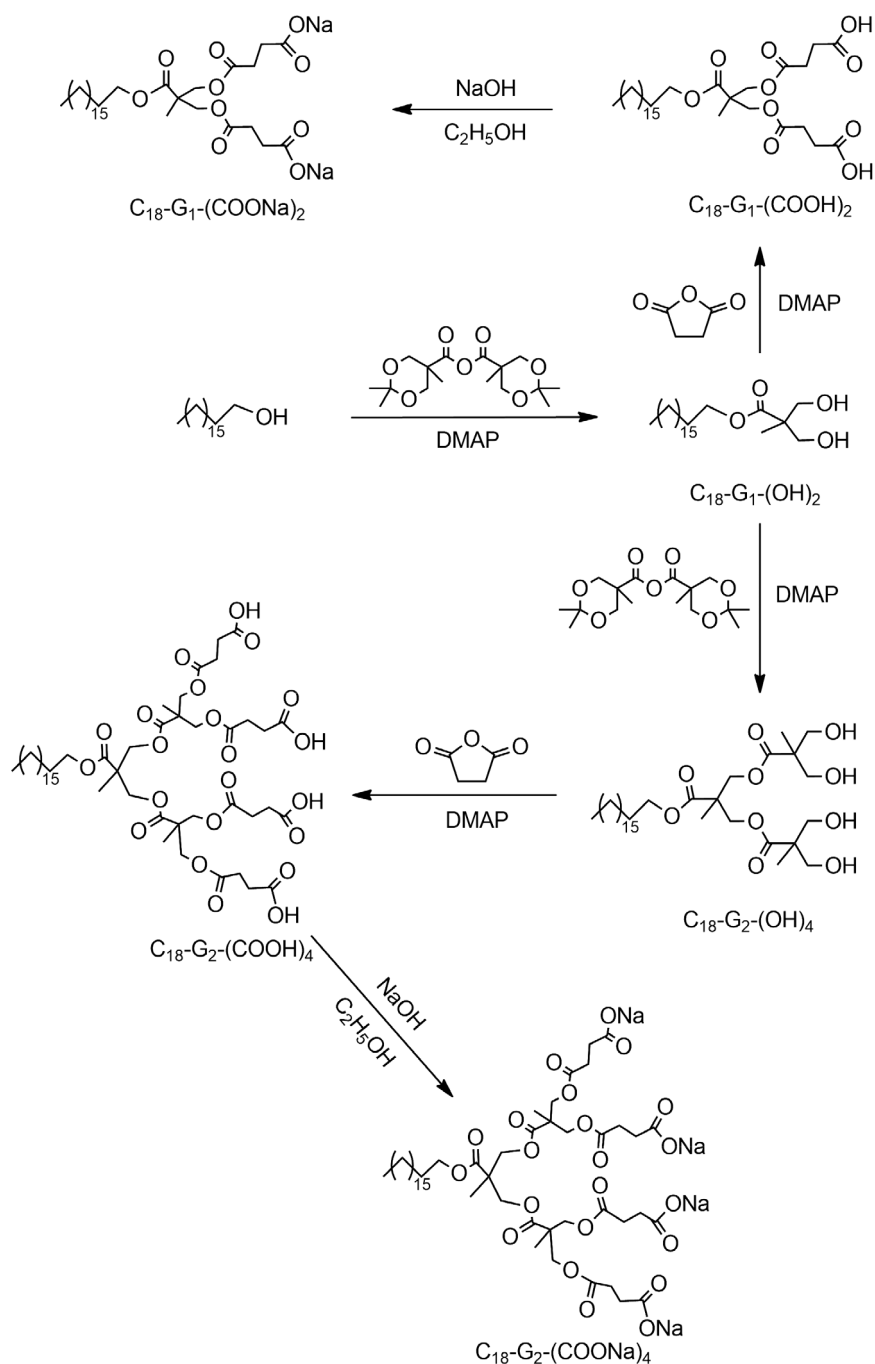
## Materials and Methods

### Materials

Sodium stearate ( $\text{C}_{18}\text{H}_{37}\text{COONa}$ , purity  $\geq 99\%$ ) was purchased from TCI (Shanghai, China) Development Co., Ltd. Sodium octadecyl sulfate ( $\text{C}_{18}\text{H}_{37}\text{OSO}_3\text{Na}$ , purity  $\geq 99\%$ ) was obtained from Acros Organics (Shanghai, China) Co., Ltd. 2,2-Bis(hydroxymethyl)propionic acid (purity  $\geq 99\%$ ) was purchased from Shanghai D&B Biological Scientific (Shanghai, China) Co., Ltd. Octadecanol (purity  $\geq 99\%$ ), succinic anhydride (purity  $\geq 99\%$ ), and 4-dimethylaminopyridine (DMAP, purity  $\geq 99\%$ ) were obtained from J&K Scientific (Shanghai, China) Co., Ltd. 2,2-dimethoxypropane (purity  $\geq 99\%$ ) and ethanol ( $\text{C}_2\text{H}_5\text{OH}$ , purity  $\geq 99\%$ ) were obtained from Sinopharm Chemical Reagent (Shanghai, China) Co., Ltd. p-Toluenesulfonic acid monohydrate (purity  $\geq 98\%$ ) was obtained from Energy Chemical (Shanghai, China) Co., Ltd. Triethylamine (purity  $\geq 99\%$ ),  $\text{N,N}'$ -dicyclohexylcarbodiimide (purity  $\geq 99\%$ ) and sodium hydroxide ( $\text{NaOH}$ , purity  $\geq 96\%$ ) was obtained from Aladdin Chemical (Shanghai, China) Co., Ltd. Silicone oil was obtained from Hangzhou Sili Organosilicone (Hangzhou, China) Co., Ltd. All other chemical reagents used were of analytical grade, and water was double distilled.

### Synthesis of Linear-Dendritic Surfactants

Two generations of linear-dendritic carboxylate surfactants  $\text{C}_{18}\text{-G}_1\text{-(COONa)}_2$  and  $\text{C}_{18}\text{-G}_2\text{-(COONa)}_4$  were synthesized using an adapted method reported in our previous work (Gong et al., 2009). As outlined in Scheme 1, the synthesis procedure is initialized by the key intermediate



**Scheme 1** Synthetic route of  $C_{18}\text{-G}_1\text{-(COONa)}_2$  and  $C_{18}\text{-G}_2\text{-(COONa)}_4$

compound of 2,2,5-trimethyl-1,3-dioxane-5-carboxylic anhydride, and followed by grafting with two or four carboxylate end groups *via* the ring-opening reaction.

Synthesis of 2,2,5-trimethyl-1,3-dioxane-5-carboxylic anhydride. 2,2,5-Trimethyl-1,3-dioxane-5-carboxylic anhydride was obtained by the dehydration of the acetonide-protected 2,2-bis(hydroxymethyl) propionic acid according

to the method described by Malkoch et al. (Malkoch et al., 2002). 2,2-Bis(hydroxymethyl)propionic acid was reacted with 2,2-dimethoxypropane and *p*-toluenesulfonic acid monohydrate in acetone for 4 h. Then the mixture was poured in triethylamine and stirred for 10 min. After removing the solvent, the dried powders were reacted with *N,N'*-dicyclohexylcarbodiimide in  $\text{CH}_2\text{Cl}_2$  for 24 h.

The product of 2,2,5-trimethyl-1,3-dioxane-5-carboxylic anhydride was finally obtained after the purification.  $^1\text{H}$  NMR ( $\text{CDCl}_3$ )  $\delta$ : 1.27 (s, 12H), 1.358 (s, 6H), 4.12–3.87 (d,  $J = 12$ , 8H).

Synthesis of  $\text{C}_{18}\text{-G}_1\text{-(OH)}_2$  and  $\text{C}_{18}\text{-G}_2\text{-(OH)}_4$ .  $\text{C}_{18}\text{-G}_1\text{-(OH)}_2$  was prepared by the method described by Würsch et al. (Würsch et al., 2001). Octadecanol and DMAP were dissolved in the mixture of water and  $\text{CH}_2\text{Cl}_2$ , and then 2,2,5-trimethyl-1,3-dioxane-5-carboxylic anhydride was added. This reaction was kept for 24 h. Then, the intermediate compound was further reacted with Dowex  $\text{H}^+$  resin in methanol for 24 h. After cooling, filtering, and concentrating, the product of  $\text{C}_{18}\text{-G}_1\text{-(OH)}_2$  was finally obtained as white crystals.  $\text{C}_{18}\text{-G}_2\text{-(OH)}_4$  was synthesized in the same way as  $\text{C}_{18}\text{-G}_1\text{-(OH)}_2$ , except the proportion of materials is different. For  $\text{C}_{18}\text{-G}_1\text{-(OH)}_2$ ,  $^1\text{H}$  NMR ( $\text{CDCl}_3$ )  $\delta$ : 0.88 (t,  $J = 8$ , 3H), 1.06 (s, 3H), 1.30 (s, 30H), 3.73 (t,  $J = 10$ , 2H), 3.89 (d,  $J = 4$ , 4H), 4.17 (t,  $J = 16$ , 2H). For  $\text{C}_{18}\text{-G}_2\text{-(OH)}_4$ ,  $^1\text{H}$  NMR ( $\text{CDCl}_3$ )  $\delta$ : 0.88 (t,  $J = 8$ , 3H), 1.05 (s, 3H), 1.27 (s, 30H), 3.72 (t,  $J = 8$ , 4H), 3.86 (d,  $J = 4$ , 8H), 4.12 (t,  $J = 16$ , 2H), 4.28–4.45 (d,  $J = 12$ , 4H).

Synthesis of  $\text{C}_{18}\text{-G}_1\text{-(COOH)}_2$  and  $\text{C}_{18}\text{-G}_2\text{-(COOH)}_4$ .  $\text{C}_{18}\text{-G}_1\text{-(COOH)}_2$  was obtained by the reaction between  $\text{C}_{18}\text{-G}_1\text{-(OH)}_2$  and succinic anhydride with the help of DMAP and triethylamine. The thin layer chromatography was used to detect the reaction process.  $\text{C}_{18}\text{-G}_2\text{-(COOH)}_4$  was synthesized from  $\text{C}_{18}\text{-G}_2\text{-(OH)}_4$  in the same way as  $\text{C}_{18}\text{-G}_1\text{-(COOH)}_2$ , except the dosage of succinic anhydride is different. For  $\text{C}_{18}\text{-G}_1\text{-(COOH)}_2$ ,  $^1\text{H}$  NMR ( $\text{CDCl}_3$ )  $\delta$ : 0.76 (t,  $J = 8$ , 3H), 1.15 (s, 3H), 1.19 (s, 30H), 1.51 (s, 2H), 2.50 (t,  $J = 4$ , 8H), 4.05 (s, 2H), 4.14 (s, 4H). For  $\text{C}_{18}\text{-G}_2\text{-(COOH)}_4$ ,  $^1\text{H}$  NMR ( $\text{CDCl}_3$ )  $\delta$ : 0.76 (t,  $J = 8$ , 3H), 1.08 (s, 9H), 1.23 (s, 30H), 1.52 (s, 2H), 2.50 (t,  $J = 4$ , 16H), 4.04 (t,  $J = 8$ , 2H), 4.12 (s, 8H).

Synthesis of  $\text{C}_{18}\text{-G}_1\text{-(COONa)}_2$  and  $\text{C}_{18}\text{-G}_2\text{-(COONa)}_4$ .  $\text{C}_{18}\text{-G}_1\text{-(COOH)}_2$  and sodium hydroxide were first dissolved in ethanol, respectively. Then, the solution of sodium hydroxide was added to  $\text{C}_{18}\text{-G}_1\text{-(COOH)}_2$  solution drop by drop.  $\text{C}_{18}\text{-G}_1\text{-(COONa)}_2$  was finally precipitated out from the solution.  $\text{C}_{18}\text{-G}_2\text{-(COONa)}_4$  is synthesized in the same way as  $\text{C}_{18}\text{-G}_1\text{-(COONa)}_2$ , except the dosage of sodium hydroxide is twice as much as  $\text{C}_{18}\text{-G}_1\text{-(COONa)}_2$ . The structures of  $\text{C}_{18}\text{-G}_1\text{-(COONa)}_2$  and  $\text{C}_{18}\text{-G}_2\text{-(COONa)}_4$  were characterized by  $^1\text{H}$  NMR and IR measurements.

### Structural Characterization

The  $^1\text{H}$  NMR spectra were recorded on a Bruker Avance 400 spectrometer ( $^1\text{H}$ , 400.00 MHz) at room temperature. The tested samples were prepared in deuterium chloroform, and tetramethylsilane was used as the internal standard. All chemical shifts ( $\delta$ ) values downfield from the signal of tetramethylsilane were given. IR spectra were obtained

on a Thermo Electron Corporation Nicolet 6700 FT-IR spectrophotometer and KBr pellets of the samples were used in analysis.

### Electrical Conductivity Measurement

The electrical conductivities of sodium stearate,  $\text{C}_{18}\text{-G}_1\text{-(COONa)}_2$ , and  $\text{C}_{18}\text{-G}_2\text{-(COONa)}_4$  solutions were measured as a function of surfactant concentration at different temperatures. A DDS-307 conductivity meter was used with a dip-type cell made of platinum black. In all experiments, the cell was partially dipped into the surfactant solution at the desired temperatures in a water bath.

### Dynamic Light Scattering Measurement

The particle size distribution of  $\text{C}_{18}\text{-G}_1\text{-(COONa)}_2$  and  $\text{C}_{18}\text{-G}_2\text{-(COONa)}_4$  micelles was determined using a Malvern Zetasizer Nano ZS at  $40^\circ\text{C}$ . The samples were filtered with a  $0.45\ \mu\text{m}$  syringe filter before test to remove the dust and other interference factors. The measurement was carried out *in situ* by dynamic light scattering with the help of Malvern Zetasizer Software v.6.34. The data of time-dependent fluctuations in the scattering intensity were treated using the cumulant analysis to estimate the diffusion coefficient, which is finally converted into the hydrodynamic diameter of the surfactant micelles according to the Stokes-Einstein equation.

### Surface Tension Measurement

The surface tensions of  $\text{C}_{18}\text{-G}_1\text{-(COONa)}_2$  and  $\text{C}_{18}\text{-G}_2\text{-(COONa)}_4$  solutions were measured as a function of surfactant concentration by a Sartorius DCAT11 tensiometer using the Wilhelmy plate method at  $40^\circ\text{C}$ . Before each measurement, the plate was firstly rinsed with double distilled water and then burned to red. For the comparability of equilibrium surface tension, the measurements were stopped when the standard deviation of the surface tension values was less than  $0.01\ \text{mN m}^{-1}$ .

### Emulsification Test

The emulsifying ability of  $\text{C}_{18}\text{-G}_1\text{-(COONa)}_2$  and  $\text{C}_{18}\text{-G}_2\text{-(COONa)}_4$  was measured in comparison with sodium stearate and sodium octadecyl sulfate. About 20 mL aqueous surfactant solution and 10 mL silicone oil were mixed under magnetic stirring for 30 min in  $40^\circ\text{C}$  water bath. Then, the emulsions were prepared through the high-speed homogenization at 10,000 rpm for 5 min using a Fluko FA25 homogenizer. The stability of emulsions was tested by observing the time for the separation of 5 mL aqueous phase from the emulsion layer.

## Statistical Analysis

Data are presented as mean and standard deviations. For all measurements, a minimum of three replicates was taken for data analysis.

## Results and Discussion

### Synthesis and Characterization of $C_{18}\text{-G}_1\text{-(COONa)}_2$ and $C_{18}\text{-G}_2\text{-(COONa)}_4$

The linear-dendritic carboxylate surfactants  $C_{18}\text{-G}_1\text{-(COONa)}_2$  and  $C_{18}\text{-G}_2\text{-(COONa)}_4$  have been synthesized from the compound of 2,2,5-trimethyl-1,3-dioxane-5-carboxylic anhydride, which was then grafted with two or four carboxylate end groups (Gong et al., 2009; Malkoch et al., 2002). Octadecanol was reacted with 2,2,5-trimethyl-1,3-dioxane-5-carboxylic anhydride to obtain  $C_{18}\text{-G}_1\text{-(OH)}_2$ , which can further react with 2,2,5-trimethyl-1,3-dioxane-5-carboxylic anhydride to obtain  $C_{18}\text{-G}_2\text{-(OH)}_4$ .  $^1\text{H}$  NMR spectra of  $C_{18}\text{-G}_1\text{-(OH)}_2$  and  $C_{18}\text{-G}_2\text{-(OH)}_4$  are given in Fig. 1. Two characteristic peaks at about 1.06 and 3.73 ppm are observed, which are respectively attributed to the signals from the hydrogens in  $-\text{CH}_3$  and  $-\text{CH}_2-$  groups linked to the quaternary carbon of linear-dendritic surfactants. The quaternary carbon can be considered as the important bifurcation group for  $C_{18}\text{-G}_1\text{-(OH)}_2$  and  $C_{18}\text{-G}_2\text{-(OH)}_4$ , which is generally seen in the  $^1\text{H}$  NMR curves of the dendritic polymeric molecules (Würsch et al., 2001). Furthermore, the peak at about 4.17 ppm, corresponding to the  $-\text{CH}_2-$  group connected with the ester group formed newly, may prove

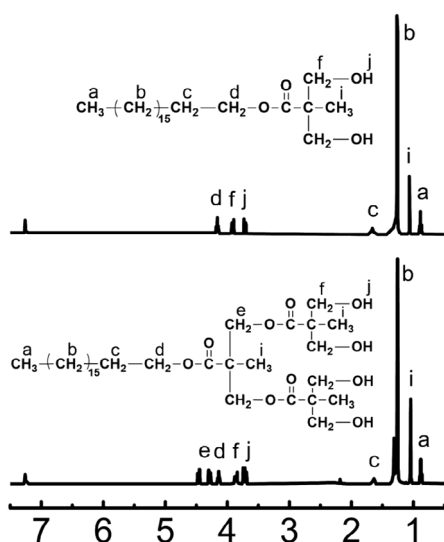


**Fig 1**  $^1\text{H}$  NMR spectra of  $C_{18}\text{-G}_1\text{-(OH)}_2$  and  $C_{18}\text{-G}_2\text{-(OH)}_4$ . The peak at 7.26 ppm is originated from the solvent  $\text{CDCl}_3$

the complete reaction of 2,2,5-trimethyl-1,3-dioxane-5-carboxylic anhydride with octadecanol and  $C_{18}\text{-G}_1\text{-(OH)}_2$ .

While  $C_{18}\text{-G}_1\text{-(COOH)}_2$  and  $C_{18}\text{-G}_2\text{-(COOH)}_4$  were synthesized by reacting  $C_{18}\text{-G}_1\text{-(OH)}_2$  and  $C_{18}\text{-G}_2\text{-(OH)}_4$  with succinic anhydride, respectively, two linear-dendritic carboxylate surfactants  $C_{18}\text{-G}_1\text{-(COONa)}_2$  and  $C_{18}\text{-G}_2\text{-(COONa)}_4$  were finally obtained by the reaction of  $C_{18}\text{-G}_1\text{-(COOH)}_2$  and  $C_{18}\text{-G}_2\text{-(COOH)}_4$  with sodium hydroxide in ethanol, respectively. Figure 2 gives the  $^1\text{H}$  NMR spectra of  $C_{18}\text{-G}_1\text{-(COONa)}_2$  and  $C_{18}\text{-G}_2\text{-(COONa)}_4$ , which are almost same as those of  $C_{18}\text{-G}_1\text{-(COOH)}_2$  and  $C_{18}\text{-G}_2\text{-(COOH)}_4$  due to nearly same chemical environments of their hydrogens. The characteristic peaks attributed to the quaternary carbon of linear-dendritic structures are reserved for  $C_{18}\text{-G}_1\text{-(COONa)}_2$  and  $C_{18}\text{-G}_2\text{-(COONa)}_4$ . Compared to the  $^1\text{H}$  NMR spectra of  $C_{18}\text{-G}_1\text{-(OH)}_2$  and  $C_{18}\text{-G}_2\text{-(OH)}_4$ , the presence of two new peaks at 2.3–2.5 ppm for  $C_{18}\text{-G}_1\text{-(COONa)}_2$  and  $C_{18}\text{-G}_2\text{-(COONa)}_4$  may give the indication of the conversion from the hydroxyl group into carboxylate group. Carboxylate and ester groups make two  $-\text{CH}_2-$  groups in the linkage have different chemical environments (Satyarthi et al., 2009; Wang et al., 2016), leading to two different  $^1\text{H}$  NMR peaks at 2.3–2.5 ppm. Moreover, the ratios of peak areas at about 0.88, 1.06, and 2.3–2.5 ppm of  $C_{18}\text{-G}_1\text{-(COONa)}_2$  and  $C_{18}\text{-G}_2\text{-(COONa)}_4$  are in well agreement with their linear-dendritic structures.

The structures of  $C_{18}\text{-G}_1\text{-(COONa)}_2$  and  $C_{18}\text{-G}_2\text{-(COONa)}_4$  can be further demonstrated by comparing their IR spectra together with that of sodium stearate, as shown in Fig. 3. All three surfactants have C–H stretching vibration bands in the region from 2800 to 3000  $\text{cm}^{-1}$  and high-intensity band at  $\sim 1570\text{ cm}^{-1}$ , which is ascribed to the stretching vibration from C=O group of carboxylates. This result is generally observed in the IR spectra of carboxylate

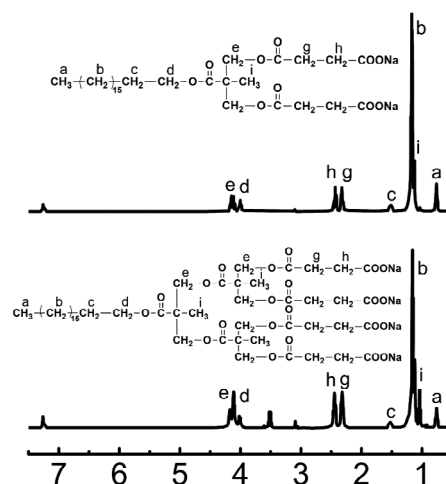


**Fig 2**  $^1\text{H}$  NMR spectra of  $C_{18}\text{-G}_1\text{-(COONa)}_2$  and  $C_{18}\text{-G}_2\text{-(COONa)}_4$ . The peak at 7.26 ppm is originated from the solvent  $\text{CDCl}_3$

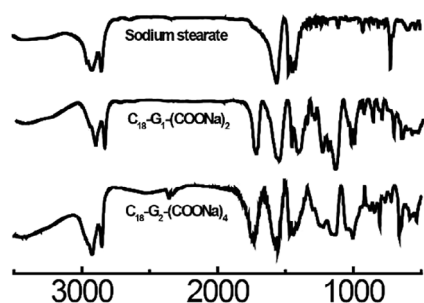


**Fig 3** IR spectra of sodium stearate,  $C_{18}\text{-G}_1\text{-(COONa)}_2$ , and  $C_{18}\text{-G}_2\text{-(COONa)}_4$

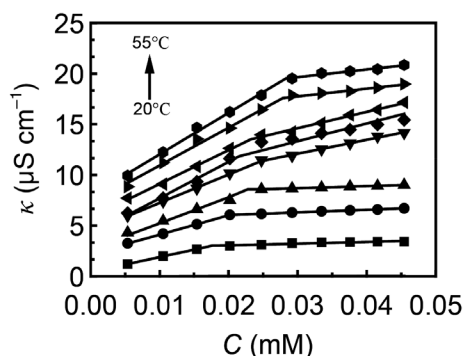


**Fig 4** Variations of the electrical conductivity as a function of the concentration of  $C_{18}\text{-G}_1\text{-(COONa)}_2$  at various temperatures

compounds of fatty acids (Bani-Jaber et al., 2012; Vaisman et al., 2013). Two new peaks at  $\sim 1740\text{ cm}^{-1}$  are observed only for  $C_{18}\text{-G}_1\text{-(COONa)}_2$  and  $C_{18}\text{-G}_2\text{-(COONa)}_4$ , which are resulted from the stretching vibration from  $\text{C}=\text{O}$  in the ester group. The existence of these two special bands further illustrates that the two generations of linear-dendritic surfactants have been successfully synthesized.

### Solubility and Micellization of Linear-Dendritic Carboxylate Surfactants

The solubility and micellization properties of  $C_{18}\text{-G}_1\text{-(COONa)}_2$  and  $C_{18}\text{-G}_2\text{-(COONa)}_4$  as well as sodium stearate have been investigated using the electrical conductivity method. Figure 4 gives the representative plots of electrical conductivity against the surfactant concentration of  $C_{18}\text{-G}_1\text{-(COONa)}_2$  at different temperatures. At low-surfactant concentrations, the electrical conductivity increases linearly with the increase of  $C_{18}\text{-G}_1\text{-(COONa)}_2$  concentration at all investigated temperatures. However, after a turning point, the electrical conductivity curve gives different changes at low and high temperatures. At low temperatures, the almost unchanged electrical conductivity values suggest that the maximum solubility is reached at the turning point (Bakshi

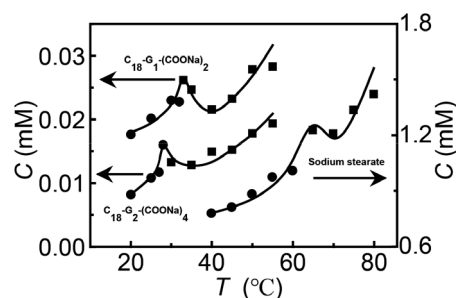


**Fig 5** Variations of the maximum solubility (circular point) and CMC (square point) of sodium stearate,  $C_{18}\text{-G}_1\text{-(COONa)}_2$ , and  $C_{18}\text{-G}_2\text{-(COONa)}_4$  as a function of temperature

et al., 2004), beyond which the surfactant is no longer dissolved in water and the electrical conductivity does not increase anymore. Because the ionic surfactants have the significantly improved solubility above the Krafft temperature, the electrical conductivity continues to increase with increasing surfactant concentration even after the turning point. At high temperatures, the turning point in the electrical conductivity curve corresponds to the CMC of the surfactant (Chauhan et al., 2012). While surfactant molecules are completely ionized below the CMC, the counterions are bound to surfactant micelles above the CMC, which subsequently causes a reduction in the slope of the electrical conductivity relative to the surfactant concentration.

Figure 5 gives the variations of the maximum solubility and CMC of sodium stearate,  $C_{18}\text{-G}_1\text{-(COONa)}_2$ , and  $C_{18}\text{-G}_2\text{-(COONa)}_4$  as a function of temperature. Determined from the interception of the two lines of maximum solubility and CMC, the Krafft temperatures of sodium stearate,  $C_{18}\text{-G}_1\text{-(COONa)}_2$ , and  $C_{18}\text{-G}_2\text{-(COONa)}_4$  are 65.2, 33.2, and 28.4°C, respectively. Sodium stearate carrying an alkyl chain with 18 carbons has high hydrophobicity, leading to the low solubility and high Krafft temperature (Nardello et al., 2006). Compared to sodium stearate, sulfate surfactant sodium octadecyl sulfate with the same alkyl chain has a smaller Krafft temperature (56.0°C), whereas sodium pentadecyl sulfate (31.5°C) and sodium tetradecyl sulfate (30.0°C) with shorter alkyl chain have much smaller Krafft temperatures (Li et al., 2005). It is clear that the Krafft temperatures of  $C_{18}\text{-G}_1\text{-(COONa)}_2$  and  $C_{18}\text{-G}_2\text{-(COONa)}_4$  are much lower than sodium stearate and sodium octadecyl sulfate, but roughly equivalent to sodium pentadecyl sulfate and sodium tetradecyl sulfate. The decreased Krafft temperatures of  $C_{18}\text{-G}_1\text{-(COONa)}_2$  and  $C_{18}\text{-G}_2\text{-(COONa)}_4$  correspond to the superior solubilities, which could be a consequence of their two and four headgroups containing carboxylate and ester groups. This result is consistent with the observation by Holmberg et al., who found the enhanced solubility for the surfactants upon increasing the

number of cationic headgroup linked with ester group (Tehrani-Bagha and Holmberg, 2010).

In agreement with the Krafft temperature data,  $C_{18}\text{-G}_1\text{-(COONa)}_2$  and  $C_{18}\text{-G}_2\text{-(COONa)}_4$  give much smaller CMC values than sodium stearate, indicating much better tendency for forming micelles. The formation of micelles is not only affected by the hydrophobic interaction between surfactant alkyl chains, but also by the intermolecular force such as the electrostatic repulsion between the surfactant headgroups, the hydrogen bonding between the surfactant headgroups and water molecules in the solution. Given that  $C_{18}\text{-G}_1\text{-(COONa)}_2$ ,  $C_{18}\text{-G}_2\text{-(COONa)}_4$ , and sodium stearate share the same linear alkyl chain, the structure of headgroup part should be the major determining factor for the micelle formation. Although the headgroups of linear-dendritic surfactants have the enhanced electrostatic repulsion compared to sodium stearate, the increase in the hydrophilicity of linear-dendritic surfactants may cause the micelle formation to be more favorable. This result is in well agreement with previous result from Garofalo et al. (2014), where a decrease of CMC by increasing the hydrophilicity of copolymers was reported. Bhattacharya et al. discussed that the ester linkages at the hydrocarbon chain-charged headgroup connection, located at the micellar stern layer region, may facilitate intermolecular association of the surfactants through dipole-induced dipolar interactions and therefore probably enhances the tendency to aggregate into surfactant micelles (Bhattacharya and Haldar, 2004). Therefore, the CMC values are more affected by the branching degree of headgroup: the CMC value of  $C_{18}\text{-G}_2\text{-(COONa)}_4$  with four headgroups is lower than that of  $C_{18}\text{-G}_1\text{-(COONa)}_2$  with two headgroups. Additionally, the CMC values of three surfactants decrease first and then increase with increasing temperature. This result is generally observed for the ionic surfactants (González-Pérez et al., 2001), owing to the different influences of temperature on the hydrations of surfactant hydrophobic and hydrophilic parts.

The formation of surfactant micelles is a spontaneous process, which is usually evaluated by the relative change in Gibbs energy of micellization ( $\Delta G$ ).  $\Delta G$  is one important thermodynamic parameter of the surfactant system, which can be calculated based on the CMC and electrical conductivity data. There are different equations to calculate  $\Delta G$  values of surfactant micellization, depending on the numbers of surfactant headgroup and alkyl chain (Franke and Rehage, 2019b; Zana, 1996). Considering the structures of headgroups, the  $\Delta G$  values of sodium stearate,  $C_{18}\text{-G}_1\text{-(COONa)}_2$ , and  $C_{18}\text{-G}_2\text{-(COONa)}_4$  can be calculated according to the Eqs 1–3, respectively.

$$\Delta G = RT(1 + \beta)\ln\text{CMC} \quad (1)$$

$$\Delta G = RT(1 + 2\beta)\ln\text{CMC} + 2RT\beta\ln 2 \quad (2)$$

$$\Delta G = RT(1 + 4\beta)\ln\text{CMC} + 4RT\beta\ln 4 \quad (3)$$

where CMC is expressed in molarity,  $R$  is the gas constant, and  $T$  is temperature on the Kelvin scale.  $\beta$  is the degree of dissociation of the micelles, which is determined from the ratio of the post-micellar slope to the pre-micellar slope in the electrical conductivity curve.

The  $\Delta G$  values of sodium stearate,  $C_{18}\text{-G}_1\text{-(COONa)}_2$ , and  $C_{18}\text{-G}_2\text{-(COONa)}_4$  at high temperatures beyond the lowest point in the CMC curves have been obtained. The average  $\Delta G$  values are 32.1, 64.3, and 100.4  $\text{kJ mol}^{-1}$ , corresponding to sodium stearate at 70–80°C,  $C_{18}\text{-G}_1\text{-(COONa)}_2$  at 45–55°C, and  $C_{18}\text{-G}_2\text{-(COONa)}_4$  at 45–55°C, respectively. All three surfactants give the negative  $\Delta G$  values, which indicate the spontaneous characteristics of the micellization process. Moreover, it is noted that the absolute values of  $\Delta G$  have the order of  $C_{18}\text{-G}_2\text{-(COONa)}_4 > C_{18}\text{-G}_1\text{-(COONa)}_2 >$  sodium stearate. Previously, Holmberg et al. found that the surfactants had smaller CMC values upon increasing the number of cationic headgroup linked with ester group (Tehrani-Bagha and Holmberg, 2010). The thermodynamic calculation from Rosen et al. also suggested that the  $\Delta G$  value becomes more negative upon the introduction of oxyethylene units into surfactant molecule (Dahanayake et al., 1986). Consistent with these reported work, our result reveals that the dendritic headgroup composed of the carboxylate and ester groups can increase the driving force for the formation of micelles, which leads to the most negative  $\Delta G$  value for  $C_{18}\text{-G}_2\text{-(COONa)}_4$ .

As shown in Fig. 6, dynamic light scattering has been used to measure the particle size distribution of  $C_{18}\text{-G}_1\text{-(COONa)}_2$  and  $C_{18}\text{-G}_2\text{-(COONa)}_4$  micelles at the surfactant

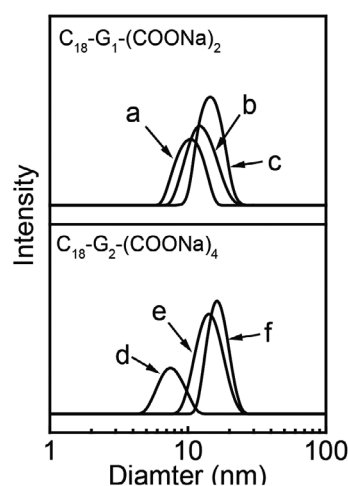


**Fig 6** Particle size distribution of  $C_{18}\text{-G}_1\text{-(COONa)}_2$  micelles (a, 0.10 mM; b, 0.15 mM; c, 0.25 mM) and  $C_{18}\text{-G}_2\text{-(COONa)}_4$  micelles (d, 0.10 mM; e, 0.15 mM; f, 0.25 mM)

concentrations of 0.10, 0.15, and 0.25 mM above the CMC values. When the surfactant concentration increases from 0.10 to 0.25 mM, the mean particle size increases from 10 to 15 nm for  $C_{18}\text{-G}_1\text{-(COONa)}_2$  and from 6 to 16 nm for  $C_{18}\text{-G}_2\text{-(COONa)}_4$ , respectively. The slightly fast increase in the mean particle size for  $C_{18}\text{-G}_2\text{-(COONa)}_4$  micelles may support the above discussion about the stronger tendency of the micelle formation for  $C_{18}\text{-G}_2\text{-(COONa)}_4$  than  $C_{18}\text{-G}_1\text{-(COONa)}_2$ . On the other hand, many people have observed the so-called sphere-to-rod micelle transition when the surfactant concentration reaches a threshold value (Christov et al., 2004; Miyagishi et al., 1996). In fact, the relatively small values of the mean particle size of  $C_{18}\text{-G}_1\text{-(COONa)}_2$  and  $C_{18}\text{-G}_2\text{-(COONa)}_4$  micelles are not as large compared with nonspherical micelles. Meanwhile, it is seen that there is no significant change in the width of particle size distribution peaks of  $C_{18}\text{-G}_1\text{-(COONa)}_2$  and  $C_{18}\text{-G}_2\text{-(COONa)}_4$  micelles. These results may indicate that  $C_{18}\text{-G}_1\text{-(COONa)}_2$  and  $C_{18}\text{-G}_2\text{-(COONa)}_4$  form spherical micelles at low surfactant concentrations (Kuperkar et al., 2010).

### Surface Activity of Linear-Dendritic Carboxylate Surfactants

Surface tension measurement is employed to evaluate the surface activity of  $C_{18}\text{-G}_1\text{-(COONa)}_2$  and  $C_{18}\text{-G}_2\text{-(COONa)}_4$ , in comparison with their corresponding carboxylic acids  $C_{18}\text{-G}_1\text{-(COOH)}_2$  and  $C_{18}\text{-G}_2\text{-(COOH)}_4$ . All

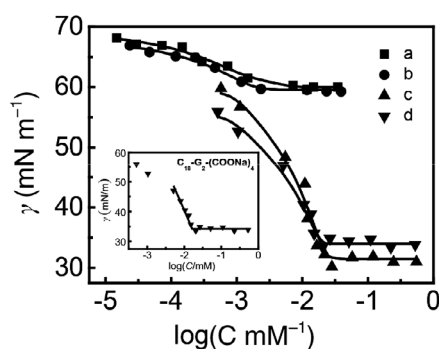


**Fig 7** Surface tension values of  $C_{18}\text{-G}_1\text{-(COOH)}_2$  (a),  $C_{18}\text{-G}_2\text{-(COOH)}_4$  (b),  $C_{18}\text{-G}_1\text{-(COONa)}_2$  (c), and  $C_{18}\text{-G}_2\text{-(COONa)}_4$  (d) as a function of surfactant concentration. The inset shows the determination of CMC using  $C_{18}\text{-G}_2\text{-(COONa)}_4$  as an example

samples are clear solutions without any precipitate, which are prepared at the concentrations quite lower than their maximum solubilities. Moreover, these samples were carefully maintained at 40°C above the Krafft temperatures of  $C_{18}\text{-G}_1\text{-(COONa)}_2$  and  $C_{18}\text{-G}_2\text{-(COONa)}_4$ . Figure 7 gives the plots of surface tension ( $\gamma$ ) versus logarithm of surfactant concentration ( $C$ ) for  $C_{18}\text{-G}_1\text{-(COOH)}_2$ ,  $C_{18}\text{-G}_2\text{-(COOH)}_4$ ,  $C_{18}\text{-G}_1\text{-(COONa)}_2$ , and  $C_{18}\text{-G}_2\text{-(COONa)}_4$  at 40°C. For four compounds, as the surfactant concentration increases, the surface tension values decrease gradually and finally achieve a relative stable value. This result suggests that both carboxylic and carboxylate types of linear-dendritic compounds can adsorb at the air/water interface. However,  $C_{18}\text{-G}_1\text{-(COONa)}_2$  and  $C_{18}\text{-G}_2\text{-(COONa)}_4$  generally have lower surface tension values than those of  $C_{18}\text{-G}_1\text{-(COOH)}_2$  and  $C_{18}\text{-G}_2\text{-(COOH)}_4$ , which indicates higher surface activity of two linear-dendritic carboxylate surfactants (Atrafi and Pawlik, 2016). It is noted that  $C_{18}\text{-G}_1\text{-(COONa)}_2$  and  $C_{18}\text{-G}_2\text{-(COONa)}_4$  give nonlinear changes in the whole surfactant concentration range below the break point in the curves of  $\gamma\text{-log}C$ , which is generally observed for the surfactant systems and can be fitted by Szyszkowski equation (Daniel and Berg, 2002). According to the common method used by other investigators (Xu et al., 2015), the CMC values of  $C_{18}\text{-G}_1\text{-(COONa)}_2$  and  $C_{18}\text{-G}_2\text{-(COONa)}_4$  are determined from the interceptions of two furnished straight lines from the linearly changed data below and above the break point, as shown in the insert in Fig. 7. The CMC values of  $C_{18}\text{-G}_1\text{-(COONa)}_2$  and  $C_{18}\text{-G}_2\text{-(COONa)}_4$  at 40°C are 0.025 and 0.017 mM respectively, as listed in Table 1. The CMC value of  $C_{18}\text{-G}_2\text{-(COONa)}_4$  is smaller than that of  $C_{18}\text{-G}_1\text{-(COONa)}_2$ , which are highly consistent with the result obtained from the electrical conductivity measurement.

As shown in Table 1, the surface tension value at the CMC ( $\gamma_{\text{CMC}}$ ) of  $C_{18}\text{-G}_2\text{-(COONa)}_4$  is higher than that of  $C_{18}\text{-G}_1\text{-(COONa)}_2$ . The ability of a surfactant to reduce the surface tension of water depends on what group it can substitute for the water at the surface and to what extent it can replace it in its ultimate adsorption. Thus, the composition of surfactant headgroup and its maximum adsorption capacity are decisive factors for reducing surface tension. Although there are more hydrophilic headgroups for  $C_{18}\text{-G}_2\text{-(COONa)}_4$ , the adsorption of  $C_{18}\text{-G}_2\text{-(COONa)}_4$  molecules at the air/water interface is somewhat hampered due to higher steric hindrance. So  $C_{18}\text{-G}_2\text{-(COONa)}_4$  is less

**Table 1** Surface activity parameters of  $C_{18}\text{-G}_1\text{-(COONa)}_2$  and  $C_{18}\text{-G}_2\text{-(COONa)}_4$

Surfactant	CMC (mM)	$\gamma_{\text{CMC}}$ (mN m <sup>-1</sup> )	$\Gamma_{\text{max}}$ ( $\mu\text{mol m}^{-2}$ )	$A_{\text{min}}$ (nm <sup>2</sup> )
$C_{18}\text{-G}_1\text{-(COONa)}_2$	0.025	31.38	3.39	0.49
$C_{18}\text{-G}_2\text{-(COONa)}_4$	0.017	34.36	0.99	1.67

capable of reducing surface tension than  $C_{18}\text{-G}_1\text{-(COONa)}_2$ . This result together with the CMC data indicates that  $C_{18}\text{-G}_2\text{-(COONa)}_4$  molecules are more inclined to aggregate into micelles in the solution than to adsorb at the air/water interface (Alexander et al., 2014; Tan et al., 2019).

The maximum surface excess ( $\Gamma_{\max}$ ) and the area occupied by a surfactant molecule ( $A_{\min}$ ) at the air/water interface are two important parameters for reflecting the adsorption amount and packing density of surfactant molecules at the air/water interface. Based on Gibbs adsorption isotherm theory (Asadov et al., 2019b), the values of  $\Gamma_{\max}$  and  $A_{\min}$  can be calculated by Eqs 4 and 5.

$$\Gamma_{\max} = - \left( \frac{1}{2.303nRT} \right) \left( \frac{d\gamma}{d\log C} \right)_T \quad (4)$$

$$A_{\min} = \frac{10^{24}}{N_A \Gamma_{\max}} \quad (5)$$

where  $\Gamma_{\max}$  is expressed in  $\mu\text{mol m}^{-2}$ ,  $A_{\min}$  is expressed in  $\text{nm}^2$ ,  $R$  is the gas constant,  $T$  is temperature on the Kelvin scale,  $\gamma$  represents the surface tension in  $\text{mN m}^{-1}$ ,  $d\gamma/d\log C$  is the slope of the linear line used for the determination of the CMC value below the break point in the  $\gamma\text{-log}C$  curve,  $N_A$  is Avogadro's number. The value of  $n$  is the number of ionic species whose adsorption amount at the interface changes along with the surfactant concentration. Considering the headgroup numbers of linear-dendritic carboxylate surfactants (Azum et al., 2016; Zana, 2002), 2 and 4 are adopted for  $n$  values of  $C_{18}\text{-G}_1\text{-(COONa)}_2$  and  $C_{18}\text{-G}_2\text{-(COONa)}_4$ , respectively.

Table 1 gives the values of  $\Gamma_{\max}$  and  $A_{\min}$  of  $C_{18}\text{-G}_1\text{-(COONa)}_2$  and  $C_{18}\text{-G}_2\text{-(COONa)}_4$ . While the values of  $\Gamma_{\max}$  of  $C_{18}\text{-G}_1\text{-(COONa)}_2$  and  $C_{18}\text{-G}_2\text{-(COONa)}_4$  are 3.39 and  $0.99 \mu\text{mol m}^{-2}$  respectively,  $C_{18}\text{-G}_1\text{-(COONa)}_2$  and  $C_{18}\text{-G}_2\text{-(COONa)}_4$  have  $A_{\min}$  values of 0.49 and  $1.67 \text{ nm}^2$ , respectively. It is noted that  $C_{18}\text{-G}_1\text{-(COONa)}_2$  has bigger  $\Gamma_{\max}$  value than  $C_{18}\text{-G}_2\text{-(COONa)}_4$ , but the  $A_{\min}$  values show the contrary variation for two linear-dendritic carboxylate surfactants. This result is consistent with the  $\Gamma_{\max}$  and  $A_{\min}$  results of other surfactant system (Azum et al., 2016).  $C_{18}\text{-G}_2\text{-(COONa)}_4$  has a large molecule volume with four headgroups to increase the steric hindrance during packing in the adsorption layer, which results in the decrease of surface adsorption amount and the increase of the area per molecule (Alexander et al., 2014). Meanwhile, when there are more hydrophilic groups in the headgroup, the surfactant can get in contact with water directly, be lying and stretching more at the air/water interface. Therefore, it is likely that  $C_{18}\text{-G}_2\text{-(COONa)}_4$  molecules are not closely packed and have lower packing density at the air/water interface.

## Emulsifying Ability of Linear-Dendritic Carboxylate Surfactants

Surfactant molecules can be absorbed at oil/water interface to create a protective barrier for reducing the physical contact between the droplets and decreasing the potential for coalescence (Noori et al., 2014). The separation time of the aqueous phase from the emulsion layer is used to measure the emulsifying ability of  $C_{18}\text{-G}_1\text{-(COONa)}_2$  and  $C_{18}\text{-G}_2\text{-(COONa)}_4$  in comparison with sodium stearate and sodium octadecyl sulfate. The stability of emulsion composed of silicone oil and water in the presence of surfactant was investigated at  $40^\circ\text{C}$ . When sodium stearate and sodium octadecyl sulfate are added, it takes 52 and 77 s, respectively, for separation of the aqueous layer from the emulsion, whereas for  $C_{18}\text{-G}_1\text{-(COONa)}_2$  and  $C_{18}\text{-G}_2\text{-(COONa)}_4$  the times taken are 84 and 106 s, respectively. The tested four surfactants have the same alkyl chain except the headgroup structure. Sodium octadecyl sulfate gives better emulsifying property than sodium stearate, which is resulted from higher charge density of sulfate headgroup of the former. Compared to two conventional surfactants,  $C_{18}\text{-G}_1\text{-(COONa)}_2$  and  $C_{18}\text{-G}_2\text{-(COONa)}_4$  have higher emulsifying ability owing to their special dendritic headgroups carrying the carboxylate and ester groups (Zhang et al., 2017).

## Conclusions

The linear-dendritic carboxylate surfactants from generation one to generation two have been synthesized and studied with respect to their solubility, micellization, and surface activity.  $C_{18}\text{-G}_1\text{-(COONa)}_2$  and  $C_{18}\text{-G}_2\text{-(COONa)}_4$  show high solubility capacity, indicated by their much smaller Krafft temperatures compared to the corresponding conventional surfactant sodium stearate. The values of CMC and  $\Delta G$  indicate that the micellizations of linear-dendritic carboxylate surfactants become more favorable with the increase in the headgroup number. On the contrary, compared to  $C_{18}\text{-G}_1\text{-(COONa)}_2$ , the surface activity parameters of  $\gamma_{\text{CMC}}$ ,  $\Gamma_{\max}$ , and  $A_{\min}$  reveal that  $C_{18}\text{-G}_2\text{-(COONa)}_4$  molecules have lower tendency to adsorb at the air/water interface. This result suggests that the increase in the number of headgroup results in lower intermolecular packing density of linear-dendritic surfactant molecules at the air/water interface, mainly due to the steric repulsions of the dendritic structure of surfactant headgroups. This work on the solubility, micellization, and surface activity of linear-dendritic carboxylate surfactants may urge us to design novel types of surfactants with special structural properties and aggregation behaviors.

**Acknowledgement** This work is supported by the National Natural Science Foundation of China (Grant 21573071).

**Conflict of Interest** The authors declare that they have no conflict of interest.

## References

- Alexander, S., Smith, G. N., James, C., Rogers, S. E., Guittard, F., Sagisaka, M., & Eastoe, J. (2014) Low-surface energy surfactants with branched hydrocarbon architectures. *Langmuir*, **30**: 3413–3421.
- Allen, F. J., Truscott, C. L., Gutfreund, P., Welbourn, R. J. L., & Clarke, S. M. (2019) Potassium, calcium, and magnesium bridging of AOT to mica at constant ionic strength. *Langmuir*, **35**: 5753–5761.
- Asadov, Z. H., Ahmadova, G. A., Rahimov, R. A., Hashimzade, S.-Z. F., Ismailov, E. H., Asadova, N. Z., ... Agamaliyeva, D. B. (2019a) Micellization and adsorption properties of new cationic gemini surfactants having hydroxyisopropyl group. *Journal of Chemical & Engineering Data*, **64**:952–962.
- Atrafi, A., & Pawlik, M. (2016) Surface tension and gas dispersion properties of fatty acid solutions. *Minerals Engineering*, **85**: 138–147.
- Azum, N., Rub, M. A., & Asiri, A. M. (2016) Micellization and interfacial behavior of the sodium salt of ibuprofen–BRIJ-58 in aqueous/brine solutions. *Journal of Solution Chemistry*, **45**: 791–803.
- Bakshi, M. S., Kaura, A., Miller, J. D., & Paruchuri, V. K. (2004) Sodium dodecyl sulfate–poly(amidoamine) interactions studied by AFM imaging, conductivity, and Krafft temperature measurements. *Journal of Colloid and Interface Science*, **278**:472–477.
- Bani-Jaber, A., Hamdan, I., & Alkawareek, M. (2012) The synthesis and characterization of fatty acid salts of chitosan as novel matrices for prolonged intragastric drug delivery. *Archives of Pharmacal Research*, **35**:1159–1168.
- Bhattacharya, S., & Haldar, J. (2004) Thermodynamics of micellization of multiheaded single-chain cationic surfactants. *Langmuir*, **20**:7940–7947.
- Bhattacharya, S., & Samanta, S. K. (2011) Surfactants possessing multiple polar heads. A perspective on their unique aggregation behavior and applications. *Journal of Physical Chemistry Letters*, **2**:914–920.
- Chauhan, S., Sharma, K., Rana, D. S., Kumar, G., & Umar, A. (2012) Conductance, apparent molar volume and compressibility studies of cetyltrimethylammonium bromide in aqueous solution of leucine. *Journal of Molecular Liquids*, **175**:103–110.
- Christov, N. C., Denkov, N. D., Kralchevsky, P. A., Ananthapadmanabhan, K. P., & Lips, A. (2004) Synergistic sphere-to-rod micelle transition in mixed solutions of sodium dodecyl sulfate and cocoamidopropyl betaine. *Langmuir*, **20**:565–571.
- Dahanayake, M., Cohen, A. W., & Rosen, M. J. (1986) Relationship of structure to properties of surfactants. 13. Surface and thermodynamic properties of some oxyethylenated sulfates and sulfonates. *The Journal of Physical Chemistry*, **90**:2413–2418.
- Daniel, R. C., & Berg, J. C. (2002) Dynamic surface tension of poly-disperse surfactant solutions: A pseudo-single-component approach. *Langmuir*, **18**:5074–5082.
- Franke, M. E., & Rehage, H. (2019a) Effects of chirality on the aggregation properties of amide-bonded pyridinium gemini surfactants. *Langmuir*, **35**:8968–8976.
- Garofalo, C., Capuano, G., Sottile, R., Talerico, R., Adami, R., Reverchon, E., ... Pappalardo, D. (2014) Different insight into amphiphilic PEG-PLA copolymers: Influence of macromolecular architecture on the micelle formation and cellular uptake. *Bio-macromolecules*, **15**:403–415.
- Gong, F., Cheng, X., Wang, S., Wang, Y., Gao, Y., & Cheng, S. (2009) Biodegradable comb-dendritic tri-block copolymers consisting of poly(ethylene glycol) and poly(L-lactide): Synthesis, characterizations, and regulation of surface morphology and cell responses. *Polymer*, **50**:2775–2785.
- González-Pérez, A., del Castillo, J. L., Czapkiewicz, J., & Rodríguez, J. R. (2001) Conductivity, density, and adiabatic compressibility of dodecyldimethylbenzylammonium chloride in aqueous solutions. *The Journal of Physical Chemistry. B*, **105**: 1720–1724.
- Gosika, M., Sen, S., Kundagrami, A., & Maiti, P. K. (2019) Understanding the thermodynamics of the binding of pamam dendrimers to graphene: A combined analytical and simulation study. *Langmuir*, **35**:9219–9232.
- Jacobs, J., Byrne, A., Gathergood, N., Keyes, T. E., Heuts, J. P. A., & Heise, A. (2014) Facile synthesis of fluorescent latex nanoparticles with selective binding properties using amphiphilic glycosylated polypeptide surfactants. *Macromolecules*, **47**:7303–7310.
- Khuwijitjaru, P., Adachi, S., & Matsuno, R. (2002) Solubility of saturated fatty acids in water at elevated temperatures. *Bioscience, Biotechnology, and Biochemistry*, **66**:1723–1726.
- Kuperkar, K., Abezgauz, L., Prasad, K., & Bahadur, P. (2010) Formation and growth of micelles in dilute aqueous CTAB solutions in the presence of NaNO<sub>3</sub> and NaClO<sub>3</sub>. *Journal of Surfactants and Detergents*, **13**:293–303.
- Li, Y., Xu, G., Luan, Y., Yuan, S., & Xin, X. (2005) Property prediction on surfactant by quantitative structure-property relationship: Krafft point and cloud point. *Journal of Dispersion Science and Technology*, **26**:799–808.
- Liu, X., Piao, X., Wang, Y., & Zhu, S. (2008) Liquid-liquid equilibrium for systems of (fatty acid ethyl esters + ethanol + soybean oil and fatty acid ethyl esters + ethanol + glycerol). *Journal of Chemical & Engineering Data*, **53**:359–362.
- Malkoch, M., Malmström, E., & Hult, A. (2002) Rapid and efficient synthesis of aliphatic ester dendrons and dendrimers. *Macromolecules*, **35**:8307–8314.
- Mirgorodskaya, A. B., Valeeva, F. G., Lukashenko, S. S., Kushnazarova, R. A., Prokopéva, T. M., Zubareva, T. M., ... Zakharova, L. Y. (2018) Dicationic hydroxylic surfactants: Aggregation behavior, guest-host interaction and catalytic effect. *Journal of Molecular Liquids*, **250**:229–235.
- Miyagishi, S., Suzuki, H., & Asakawa, T. (1996) Microviscosity and aggregation number of potassium N-acylalaninate micelles in potassium chloride solution. *Langmuir*, **12**:2900–2905.
- Nardello, V., Chailloux, N., Joly, G., & Aubry, J.-M. (2006) Preparation, amphiphilic properties and lyotropic phase behaviour of new surfactants based on sodium monoalkyl  $\alpha,\omega$ -dicarboxylates. *Colloids and Surfaces, A: Physicochemical and Engineering Aspects*, **288**:86–95.
- Naves, A. F., Palombo, R. R., Carrasco, L. D. M., & Carmona-Ribeiro, A. M. (2013) Antimicrobial particles from emulsion polymerization of methyl methacrylate in the presence of quaternary ammonium surfactants. *Langmuir*, **29**:9677–9684.
- Noori, S., Naqvi, A. Z., Ansari, W. H., Akram, M., & Kabir-ud-Din (2014) Synthesis and investigation of surface active properties of counterion coupled gemini surfactants. *Journal of Surfactants and Detergents*, **17**:409–417.
- Satyarthi, J. K., Srinivas, D., & Ratnasamy, P. (2009) Estimation of free fatty acid content in oils, fats, and biodiesel by <sup>1</sup>H NMR spectroscopy. *Energy & Fuels*, **23**:2273–2277.
- Shavykin, O. V., Leermakers, F. A. M., Neelov, I. M., & Darinskii, A. A. (2018) Self-assembly of lysine-based dendritic surfactants modeled by the self-consistent field approach. *Langmuir*, **34**:1613–1626.

- Suek, N. W., & Lamm, M. H. (2008) Computer simulation of architectural and molecular weight effects on the assembly of amphiphilic linear-dendritic block copolymers in solution. *Langmuir*, **24**: 3030–3036.
- Tan, J., Xiong, X., He, Z., Cao, F., & Sun, D. (2019) Aggregation behavior of polyether based siloxane surfactants in aqueous solutions: Effect of alkyl groups and steric hindrance. *The Journal of Physical Chemistry. B*, **123**:1390–1399.
- Tehrani-Bagha, A. R., & Holmberg, K. (2010) Cationic ester-containing gemini surfactants: Physical–chemical properties. *Langmuir*, **26**:9276–9282.
- Tian, F., Lin, X., Valle, R. P., Zuo, Y. Y., & Gu, N. (2019) Poly (amidoamine) dendrimer as a respiratory nanocarrier: Insights from experiments and molecular dynamics simulations. *Langmuir*, **35**: 5364–5371.
- Vaisman, B., Ickowicz, D. E., Abteu, E., Haim-Zada, M., Shikanov, A., & Domb, A. J. (2013) In vivo degradation and elimination of injectable ricinoleic acid based poly(ester-anhydride). *Biomacromolecules*, **14**:1465–1473.
- Voutsas, E. C., Tsavas, P., Magoulas, K., Tassios, D., Ferrer, M., Plou, F. J., & Ballesteros, A. (2002) Solubility measurements of fatty acid glucose and sucrose esters in 2-methyl-2-butanol and mixtures of 2-methyl-2-butanol with dimethyl sulfoxide. *Journal of Chemical & Engineering Data*, **47**:1517–1520.
- Wang, H., Hamilton, M., & Rempel, G. L. (2016) Hydrogenation of sodium oleate in aqueous emulsion with the hoveyda–grubbs second-generation catalyst. *Organic Process Research and Development*, **20**:1252–1257.
- Wang, W., Lu, W., & Jiang, L. (2008) Influence of pH on the aggregation morphology of a novel surfactant with single hydrocarbon chain and multi-amine headgroups. *The Journal of Physical Chemistry. B*, **112**:1409–1413.
- Würsch, A., Möller, M., Glauser, T., Lim, L. S., Voytek, S. B., Hedrick, J. L., ... Hilborn, J. G. (2001) Dendritic-linear A<sub>x</sub>B<sub>x</sub> block copolymers prepared via controlled ring-opening polymerization of lactones from orthogonally protected multifunctional initiators. *Macromolecules*, **34**:6601–6615.
- Xu, W., Gu, H., Zhu, X., Zhong, Y., Jiang, L., Xu, M., ... Hao, J. (2015) CO<sub>2</sub>-controllable foaming and emulsification properties of the stearic acid soap systems. *Langmuir*, **31**:5758–5766.
- Zaidi, A., Alsvik, I. L., Øpstad, C. L., Martin, D., Rebman, E., Voss, G., ... Partali, V. (2018) Forgotten fatty acids—Surface properties supply conclusive evidence for including carotenoic acids. *Chemistry and Physics of Lipids*, **216**:48–53.
- Zana, R. (1996) Critical micellization concentration of surfactants in aqueous solution and free energy of micellization. *Langmuir*, **12**: 1208–1211.
- Zana, R. (2002) Dimeric and oligomeric surfactants. Behavior at interfaces and in aqueous solution: A review. *Advances in Colloid and Interface Science*, **97**:205–253.
- Zhang, R., Cai, Y., Wang, J., Zhao, Z., Mao, X., & Peng, Z. (2017) A star-shaped anionic surfactant: Synthesis, alkalinity resistance, interfacial tension and emulsification properties at the crude oil-water interface. *Journal of Surfactants and Detergents*, **20**: 1027–1035.